Effects of Shear Strain on the Conduction Band in Silicon: An Efficient Two-Band k·p Theory

Viktor Sverdlov, Enzo Ungersboeck, Hans Kosina, and Siegfried Selberherr
Institute for Microelectronics, Technische Universität Wien
Gusshausstrasse 27–29, A-1040 Vienna, Austria
Email: {sverdlov|ungersboeck|kosina|selberherr}@iue.tuwien.ac.at

Abstract— **We present an efficient two-band k·p theory which accurately describes the six lowest conduction band valleys in silicon. By comparing the model with full band pseudo-potential calculations we demonstrate that the model captures both the nonparabolicty effects and the stress-induced band structure modification for general stress conditions. It reproduces the stress dependence of the effective masses and the nonparabolicity parameter. Analytical expressions for the valley shifts and the transversal and longitudinal effective mass modifications induced by uniaxial $[110]$ stress are obtained and analyzed. The low-field mobility enhancement in the direction of tensile $[110]$ stress in $\{001\}$ SOI FETs with arbitrary small body thickness is due to a modification of the conductivity mass and is shown to be partly hampered by an increase in nonparabolicity at high stress value.**

I. INTRODUCTION

The $\mathbf{k}\cdot\mathbf{p}$ theory is a well established tool to describe the band structure analytically. After the pioneering work by Luttinger and Kohn [1] the six-band $\mathbf{k}\cdot\mathbf{p}$ method has become a standard approach to model the valence band in Si. However, the conduction band in Si is usually approximated by three pairs of equivalent minima located close to the X-points of the Brillouin zone. It is commonly assumed that close to the minima the electron dispersion is well described by the effective mass approximation. The nonparabolicity parameter $\alpha = 0.5$ eV^{-1} is introduced to describe deviations in the density of states from the purely parabolic expression, which become pronounced at higher electron energies. In ultra-thin body (UTB) FETs, however, the band nonparabolicity affects the subband quantization energies substantially, and it was recently indicated that anisotropic, direction-dependent nonparabolicity can explain the mobility behavior at high carrier concentrations in a FET with (110) UTB orientation [2]. Therefore, a more refined description of the conduction band minima beyond the usual nonparabolic approximation is needed. Another reason to challenge the standard description of the conduction band based on a single-band nonparabolic approximation is its inability to properly address the band structure modification under stress.

Stress-induced mobility enhancement in Si has become a key technique to increase performance of modern CMOS devices. In biaxially stressed devices the electron mobility can be nearly doubled. The reason for the mobility enhancement lies in the stress-induced band structure modification. The degeneracy between the six equivalent valleys is lifted due to stress-induced valley shifts. This reduces inter-valley scattering. In case of tensile biaxial stress applied in the $\{100\}$ plane the four in-plane valleys move up in energy and become de-populated. The two populated out-of-plane valleys have favorable conductivity masses, which together with reduced inter-valley scattering results in the observed mobility increase [3]. Biaxial stress is naturally introduced by growing Si epitaxially on SiGe. This method, however, requires a substantial modification of the CMOS fabrication process and is not used in mass production. Instead, semiconductor industry is exploiting techniques compatible with existing CMOS process technology. Stress in the channel is created by local stressors and/or additional cap layers. Although already successfully used in mass production, the technologically relevant case of stress along $[110]$ has received little attention within the research community. Only recently a systematic experimental study of the mobility modification due to $[110]$ stress was performed [4]. It was shown that, contrary to $[100]$ uniaxial stress, the electron mobility data for $[110]$ stress suggest that the conductivity mass depends on stress. This conclusion was also supported by recent results of pseudo-potential band structure calculations [4], [5]. Any dependence of the effective masses on stress is neglected within the standard description of the conduction band and can only be introduced phenomenologically. In order to describe the dependence of the effective mass on stress a single-band description is not sufficient, and coupling to other bands has to be taken into account.

Recently, a 30 bands $\mathbf{k}\cdot\mathbf{p}$ theory was introduced [6]. Although universal, it cannot provide an explicit analytical solution for the energy dispersion. In this work we present an efficient two-band $\mathbf{k}\cdot\mathbf{p}$ theory. By comparing our results with predictions of the pseudo-potential band structure calculations we demonstrate that the theory accurately describes both the nonparabolicty effects and the stress induced band structure modification for general stress conditions. It accurately reproduces the stress dependence of the effective mass and of the nonparabolicity parameter. The analytical two-band $\mathbf{k}\cdot\mathbf{p}$ model allows one to study the influence of the conduction band structure on transport properties of stressed FETs for general UTB orientations.

II. THEORY

We consider the pair of equivalent conduction band valleys along the $[001]$ direction. Other valleys can be analyzed

1-4244-1124-6/07/$25.00 ©2007 IEEE.

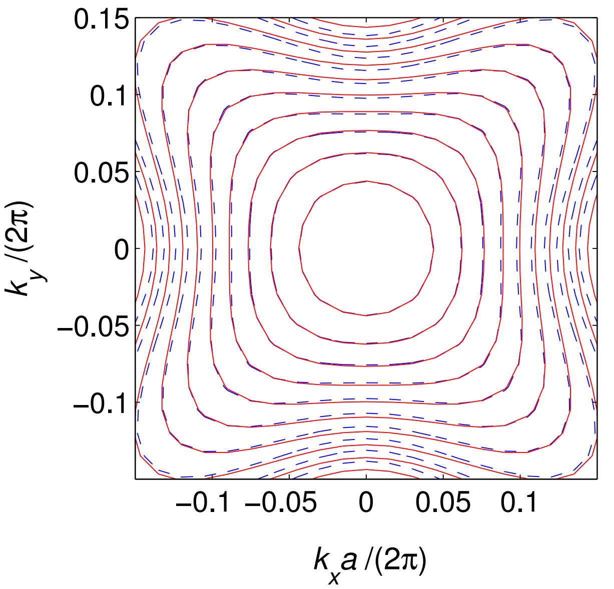

Fig. 1. [001] valley band structure obtained from EPM calculations (lines) and the analytical expression (3) (dotted lines) at $k_z = -k_0$. The distance between contour lines is 50 meV. Nonparabolicity is strongly direction dependent.

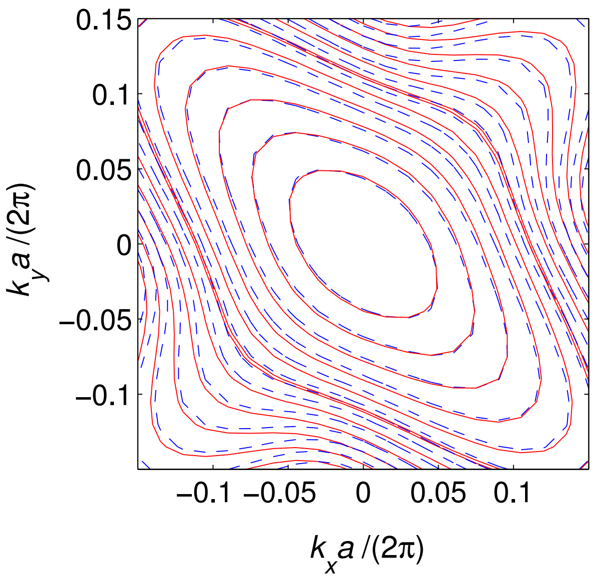

Fig. 2. [001] valley band structure obtained from EPM calculations (lines) and the analytical expression (6) (dotted lines) at $k_z = k_{\min}$, for tensile [110] uniaxial stress of 3 GPa. The distance between the contour lines is 50 meV. Strong stress-induced anisotropy in the transversal mass is observed.

analogously.

A. *Two-band* **k·p** *theory*

The closest band to the first conduction band Δ_1 ($i = 1$), which we take into account, is the second conduction band $\Delta_{2'}$ ($i = 2$). These two bands become degenerate exactly at the X point. Since the minimum of the conduction band is only $k_0 = 0.15\frac{2\pi}{a}$ away from the X point, the dispersion around the minimum can be well described by degenerate perturbation theory, which only includes the two bands degenerate at the X point. Diagonal elements of the Hamiltonian $H_{ii}, i = 1, 2$ can be easily obtained using the standard **k·p** theory:

$$H^0_{ii}(k) = (-1)^{i-1}\frac{\hbar}{m_0}k_z p + \frac{\hbar^2 k_z^2}{2m_l} + \frac{\hbar^2 k_x^2}{2m_t} + \frac{\hbar^2 k_y^2}{2m_t}, \tag{1}$$

where m_0 is the free electron mass, m_t is the transversal, and m_l is the longitudinal effective mass. Here we took into account that the matrix elements $(p_z)_{ii}$ are different only in sign, which is positive for the lower band: $p = (p_z)_{11} = -(p_z)_{22}$. The values of k_z are negative since they are counted from the X point. In contrast to the 30 bands **k·p** theory, which is developed around the Γ point far away from the conduction band minimum [6], our perturbation analysis at the X point allows to get excellent results with only two bands. Taking into account the diagonal elements (1), we recover the commonly used dispersion for the conduction band (the linear term vanishes at the minimum $k_z = -k_0$). The coupling between the bands is described by the off-diagonal terms which up to the second order are:

$$H^0_{12}(k) = \frac{\hbar^2 k_x k_y}{M}. \tag{2}$$

The parameter M is obtained from **k·p** perturbation theory [7]:

$$\frac{1}{M} = \frac{2}{m_0}\left|\sum_{l\neq i,j}\frac{(p_y)_{1l}(p_z)_{l2}}{E_k(X) - E_{\Delta_1}(X)}\right|.$$

Using degenerate perturbation theory, we find the following dispersion relation close to the minimum at $k_z = -k_0$:

$$\begin{aligned} E_0(\mathbf{k}) = \; & \tfrac{\hbar^2(\delta k_z)^2}{2m_l} + \tfrac{\hbar^2(k_x^2+k_y^2)}{2m_t} \\ & -\tfrac{\Delta}{2}\left(\left[1 + \left(\tfrac{2\hbar^2 k_x k_y}{M\Delta}\right)^2\right]^{1/2} - 1\right), \end{aligned} \tag{3}$$

where $\delta k_z = k_z + k_0$, $\Delta = 2\hbar k_0 p/m_0$ is the gap between the Δ_1 and the $\Delta_{2'}$ conduction bands at $k_z = -k_0$. In Fig. 1 this analytical expression (dotted contour lines) is compared to the numerical band structure obtained from the empirical pseudo-potential method (EPM) for $k_z = -k_0$. Excellent agreement is found up to an energy of 0.5 eV. Fig. 1 demonstrates strong anisotropy in the nonparabolicity parameter, as anticipated in [2].

B. *Stress*

In order to account for stress in our model we consider again the valley along the [001] direction. For general stress conditions the following shift in energy is added to the diagonal matrix elements (1) [8]:

$$H_{ii} = H^0_{ii} + \delta E_C, \tag{4}$$

where $\delta E_C = \Xi_d\ (\varepsilon_{xx}+\varepsilon_{yy}+\varepsilon_{zz}) + \Xi_u\ \varepsilon_{zz}$, with Ξ_d denoting the dilation and Ξ_u the uniaxial deformation potentials for the conduction band. The $\varepsilon_{ll}, l = x, y, z$ are the diagonal components of the strain tensor expressed in the principal coordinate system. The off-diagonal elements of the Hamiltonian are also modified by strain [7]:

$$H_{ij}(k) = H^0_{ij} - D\varepsilon_{xy}, \tag{5}$$

where $D \geq 0$ denotes the deformation potential for the off-diagonal strain component. When the off-diagonal components in the Hamiltonian are ignored, the influence of the shear stress component is completely lost. The off-diagonal elements of the strain tensor are, however, generated by [110] uniaxial stress. Since this is exactly the stress direction used to enhance the performance of modern MOSFETs, shear strain must be taken into consideration. The dispersion relation of the [001] valleys including the shear strain component for the conduction band now reads as:

$$E(\mathbf{k}) = \frac{\hbar^2 k_z^2}{2m_l} + \frac{\hbar^2(k_x^2+k_y^2)}{2m_t} + \delta E_C - \left[\left(\frac{\hbar}{m_0}k_z p\right)^2 + \left(D\varepsilon_{xy} - \frac{\hbar^2 k_x k_y}{M}\right)^2\right]^{1/2}, \qquad (6)$$

where the value of ε_{xy} is positive for tensile stress in [110] direction. In Fig. 2 the analytical band structure (6) is compared with the results of the EPM calculations for uniaxial [110] tensile stress of 3 GPa. Even for such large stress values the agreement between the analytical model and the numerical EPM results is excellent up to 200 meV. The band structure shown in Fig. 2 suggests a strong effective mass modification, which is analyzed in more details in the next section.

III. CONDUCTION BAND MODIFICATION DUE TO SHEAR STRAIN

The usually ignored off-diagonal strain component lifts the degeneracy between the two lowest conduction bands at the X points along the [001] axis in the Brillouin zone [7]. This lifting of degeneracy has a strong effect on the band structure. We investigate the shifts of the valley minima, changes in the effective masses and in the nonparabolicity parameter.

A. *Valley shifts*

Since the conduction band minimum along the [001] axis is located near the X point, the gap opening at the X point affects the position of the minimum. First, the conduction band minimum $k_{\min}$ moves closer to the X point. From (6) we obtain

$$k_{\min} = -k_0\sqrt{1-\eta^2}. \qquad (7)$$

Here, the dimensionless off-diagonal strain $\eta = 2D\varepsilon_{xy}/\Delta$ is introduced. For $\eta \geq 1$ the conduction band minimum is located exactly at the X point.

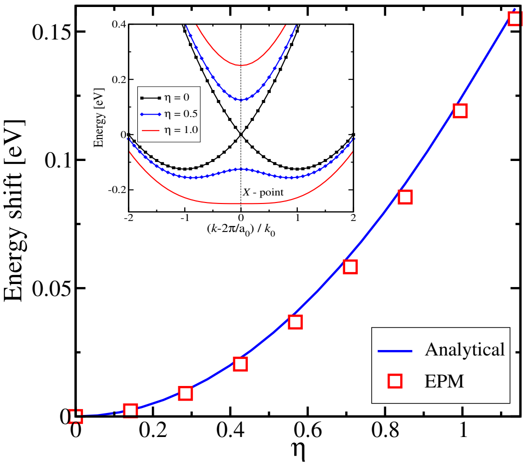

Fig. 3. [001] valley energy shift as function of the dimensionless off-diagonal component of the strain tensor, as predicted by (8) and by EPM calculations. Inset: conduction band profile along the [001] direction for different stress values.

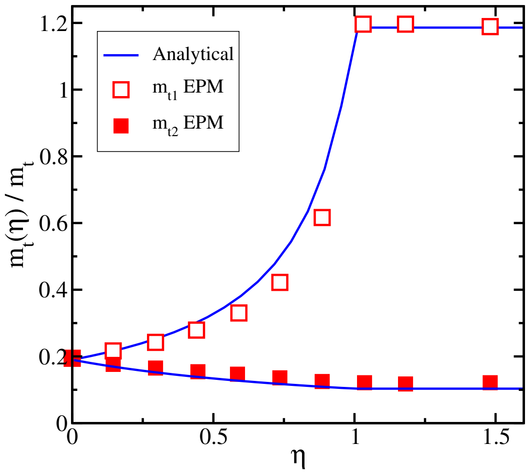

Fig. 4. Dependence of the [001] valley transversal effective mass on the dimensionless [110] uniaxial strain as predicted by (9,10) (lines) and EPM calculations (symbols). Shear stress generates strong anisotropy in the transversal masses .

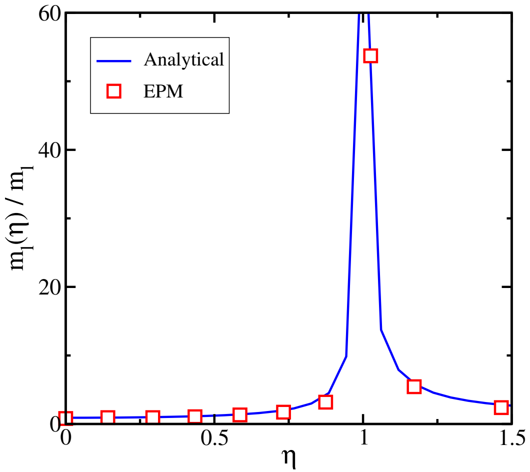

Fig. 5. Stress dependence of longitudinal effective mass in the [001] valleys due to [110] stress. Effective mass diverges at $\eta = 1$ suggesting that full-band theory must be used for such stress values.

The minima of the two [001] valleys move down in energy with respect to the remaining four fold degenerate valleys. For $\eta \leq 1$ the strain dependence is quadratic, while it is linear for $\eta \geq 1$:

$$\Delta E_{\text{shear}} = \begin{cases} -\frac{\Delta}{4}\eta^2 & , \quad |\eta| < 1 \\ -(2|\eta|-1)\Delta/4 & , \quad |\eta| > 1 \end{cases} \qquad (8)$$

In Fig. 3 the shifts predicted by (8) are compared with results from EPM calculations. Excellent agreement is found.

B. *Stress dependent effective masses*

Shear strain modifies the effective masses in the [001] valleys. Evaluating the corresponding second derivatives of (6) at the band minimum (7), we obtain two different branches for the effective mass across (m_{t1}) and along (m_{t2}) the stress direction:

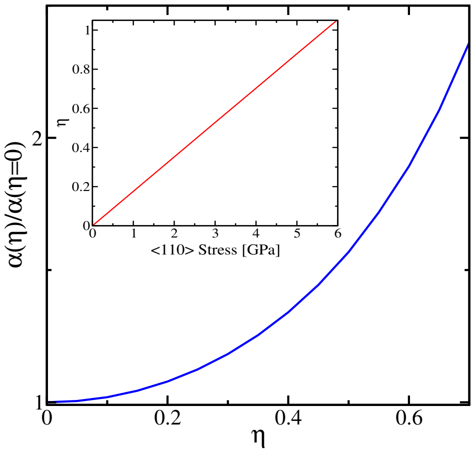

Fig. 6. Nonparabolicity parameter in the [001] valleys increases as function of [110] tensile stress. Inset: Relation between dimensionless strain η and stress in GPa.

$$m_{t1}(\eta)/m_t = \begin{cases} (1-\eta\frac{m_t}{M})^{-1} & , \quad |\eta| < 1 \\ (1-\mathrm{sgn}(\eta)\frac{m_t}{M})^{-1} & , \quad |\eta| > 1 \end{cases} \tag{9}$$

$$m_{t2}(\eta)/m_t = \begin{cases} (1+\eta\frac{m_t}{M})^{-1} & , \quad |\eta| < 1 \\ (1+\mathrm{sgn}(\eta)\frac{m_t}{M})^{-1} & , \quad |\eta| > 1 \end{cases} \tag{10}$$

Here, sgn denotes the sign function. The analytical expressions for the transversal masses (9) and (10) are compared with the masses obtained from EPM calculations in Fig. 4. Strong anisotropy in the transversal masses generated by shear strain is predicted by the analytical model.

For the longitudinal effective mass one obtains the following expression from (6):

$$m_l(\eta)/m_l = \begin{cases} (1-\eta^2)^{-1} & , \quad |\eta| < 1 \\ (1-1/|\eta|)^{-1} & , \quad |\eta| > 1 \end{cases} \tag{11}$$

Eq.(11) is compared with EPM results in Fig. 5. The longitudinal mass diverges at $\eta = 1$ suggesting that a full-band description is necessary for such high stress values [9].

C. Stress and nonparabolicity

Shear strain affects the value of the nonparabolicity parameter α. Proceeding as in [10], we arrive at an expression for the strain dependence of α:

$$\alpha(\eta) = \alpha_0 \frac{1+2(\eta m_t/M)^2}{1-(\eta m_t/M)^2} \tag{12}$$

Expression (12) is plotted in Fig. 6. The relative increase of $\alpha(\eta)$ is important at large stress values. Results of the mobility simulations in a strained ultra-thin body FET along the [110] stress direction, with and without stress dependence of the the nonparabiolicity parameter taken into account, are shown in Fig. 7. The stress dependence of the nonparabolicity parameter results in an almost 25% decrease to the mobility enhancement in a 3 nm thick SOI FET at a stress level of 3 GPa (Fig. 7). For stress values larger than 3 GPa the energy difference from the minimum to the value at the X point becomes smaller than $k_B T$, and a full-band description is required [9].

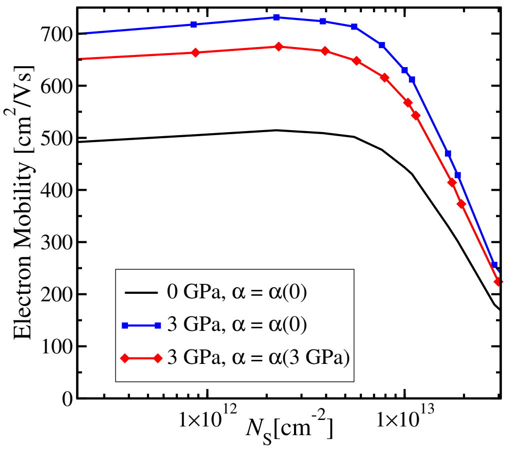

Fig. 7. [110] channel mobility in a 3 nm thick UTB FET at 3 GPa tensile stress along the channel. Mobility is computed with $\alpha = \alpha_0$ and $\alpha = \alpha(\eta)$.

IV. CONCLUSION

An efficient two-band $\mathbf{k}\cdot\mathbf{p}$ model is presented, which accurately describes the conduction band minima in strained silicon. The model accurately describes stress dependences of the effective mass and of the nonparabolicity parameter. Analytical dependences of the valley shifts, transversal and longitudinal effective masses, and the nonparabolicity parameter on shear strain are obtained and analyzed. It is demonstrated that the enhancement of low-field mobility in uniaxially stressed UTB FETs is partly hampered by an increase in nonparabolicity at higher stress.

We gratefully acknowledge financial support from the Austrian Science Fund FWF, project P19997-N14.

REFERENCES

[1] J. M. Luttinger and W. Kohn, "Motion of electrons and holes in perturbed periodic fields," *Physical Review*, vol. 97, no. 4, pp. 869–883, 1955.

[2] K. Uchida, A. Kinoshita, and M. Saitoh, "Carrier transport in (110) nMOSFETs: Subband structure, non-parabolicity, mobility characteristics, and uniaxial stress engineering," in *IEDM Techn. Dig.*, 2006, pp. 1019–1021.

[3] S. I. Takagi, J. L. Hoyt, J. J. Welser, and J. F. Gibbons, "Comparative study of phonon-limited mobility of two-dimensional electrons in strained and unstrained Si metal-oxide-semiconductor field-effect transistors," *J.Appl.Phys.*, vol. 80, no. 3, pp. 1567–1577, 1996.

[4] K. Uchida, T. Krishnamohan, K. C. Saraswat, and Y. Nishi, "Physical mechanisms of electron mobility enhancement in uniaxial stressed MOSFETs and impact of uniaxial stress engineering in ballistic regime," in *IEDM Techn. Dig.*, 2005, pp. 129–132.

[5] E. Ungersboeck, V. Sverdlov, H. Kosina, and H. Kosina, "Electron inversion layer mobility enhancement by uniaxial stress on (001) and (100) oriented MOSFETs," in *International Conference on Simulation of Semiconductor Processes and Devices*, 2006, pp. 43–46.

[6] D. Rideau, M. Feraille, L. Ciampolini, M. Minondo, C. Tavernier, H. Jaouen, and A. Ghetti, "Strained Si, Ge, and $\mathrm{Si}_{1-x}\mathrm{Ge}_x$ alloys modeled with a first-principles-optimized full-zone $\mathbf{k}\cdot\mathbf{p}$ method," *Phys. Rev. B*, vol. 74, no. 19, p. 195208, Nov 2006.

[7] J. C. Hensel, H. Hasegawa, and M. Nakayama, "Cyclotron resonance in uniaxially stressed silicon. II. Nature of the covalent bond," *Phys. Rev.*, vol. 138, no. 1A, pp. A225–A238, Apr 1965.

[8] I. Balslev, "Influence of uniaxial stress on the indirect absorption edge in Silicon and Germanium," *Physical Review*, vol. 143, pp. 636–647, 1966.

[9] E. Ungersboeck, S. Dhar, G. Karlowatz, V. Sverdlov, H. Kosina, and S. Selberherr, "The effect of general strain on band structure and electron mobility of silicon," *IEEE Trans.Electron Devices*, submitted, 2007.

[10] C. Jacoboni and L. Reggiani, "The Monte Carlo method for the solution of charge transport in semiconductors with applications to covalent materials," *Reviews of Modern Physics*, vol. 55, no. 3, pp. 645–705, 1983.